

The Transient Regime of a Multiwavelength Pyrometer¹

P. Coppa,² Dai Jinmin,³ and G. Ruffino^{2,4}

The transient operation of a new multiwavelength pyrometer based on a dispersing prism and a Si photodiode array is presented. After calibration, transient tests were performed using a tungsten strip lamp, supplied by a current pulse of 0.3-s duration. Measurements were carried out with a data acquisition system consisting of a FET multiplexer, a DVM (14 bit, 100 kHz), and a buffer memory (64 kbytes). Pyrometer signals are processed off-line, and temperature vs time is displayed. With the present arrangement, temperature measurements at 20 wavelengths may be performed with 200 μ s resolution. Faster measurements are possible with a reduced number of channels.

KEY WORDS: high-speed measurements; multiwavelength pyrometry; transient temperature measurements.

1. INTRODUCTION

A new type of multiwavelength pyrometer has been designed at the University of Rome "Tor Vergata" (Italy) [1] and built at the Harbin Institute of Technology (China). Details of the construction and steady-state operation were described previously [2]. The essential features of the instrument are presented in Fig. 1. Radiation emitted by the target T is focused by lens L_1 on a rectangular field stop D located in the focal plane of collimating lens L_2 . The parallel beam generated by the collimator is dispersed by prism P. A telescopic lens L_3 focuses the field stop in its focal plane, one image for each wavelength. An array of rectangular photodiodes, A, is

¹ Paper presented at the Third Workshop on Subsecond Thermophysics, September 17–18, 1992, Graz, Austria.

² Department of Mechanical Engineering, University of Rome "Tor Vergata," Via della Ricerca Scientifica, 00133 Rome, Italy.

³ Department of Precise Instruments, Harbin Institute of Technology, Harbin, China.

⁴ Deceased.

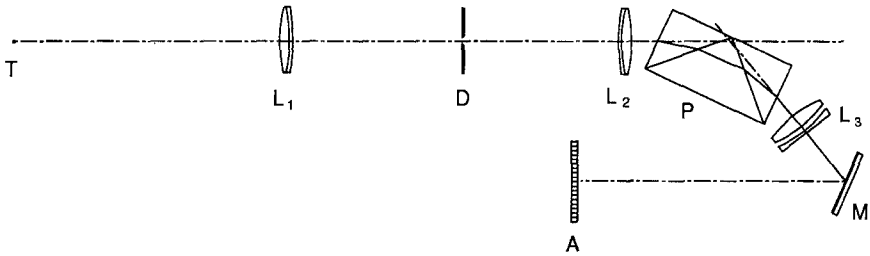


Fig. 1. Schematic diagram of the optical system.

located in this plane. If the dimensions and position of the field stop are such that each diode is its conjugate, it detects a particular band, defined by its dimensions, the focal length of the telescopic lens, the refractive indexes of the prism glasses, and the orientation of the prism. This definition is sharper and intrinsically more stable than the one achieved with interference filters.

The most relevant optical specifications are as follows: object distance from front lens, 600 mm; object size, 0.90×1.80 mm; magnification of lens L_1 , $-\frac{1}{2}$; field stop size, 0.45×0.9 mm; and magnification of lenses L_2 and L_3 , -2 .

2. ELECTRONIC DESIGN

The diodes in the array are chosen to operate in the photoconductive mode and, therefore, are connected to transconductance amplifiers (Fig. 2). Diodes are numbered in the order of decreasing wavelengths. At shorter wavelengths they are affected by two adverse facts: (a) they collect less radiation flux because the prism dispersion decreases with wavelength; and (b) at a constant temperature, below the Wien peak, the source radiance decreases with wavelength.

These inconveniences are overcome by two measures: (1) at short wavelengths, diodes are grouped, with parallel connections to the amplifier inputs; and (2) different gains are assigned to the amplifiers by appropriate feedback resistors.

Groupings and gains are selected according to the pragmatic criterion of balancing, as much as possible, for each channel, the ranges and the amplified signals at a reference temperature (the freezing point of gold, 1337.54 K, has been chosen according to a prescription of ITS-90). The resulting configuration is represented in Fig. 2. Mid wavelengths and bands, for each channel, are listed in the second and third columns in Table I.

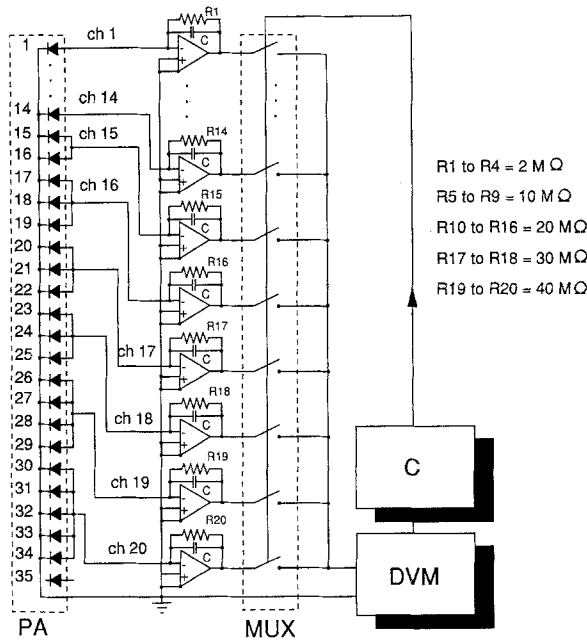


Fig. 2. Diagram of the electronic circuit of the multiwavelength pyrometer.

The array is mounted on a precisely positionable card and the diodes are connected, via shielded cables, to a mother board, where the parallel connections are made. Two side connectors hold two amplifier cards, in which the high-stability feedback resistors are mounted. This setup allows easy service and compactness, so that the entire circuit and its power supply ($\pm 15 \text{ V}$) are enclosed in the pyrometer casing.

Operational amplifiers and circuit parameters are chosen to meet the experimental requirements. We intend to apply the pyrometer to measure temperature pulses of ca. 0.3-s width. If there are no singular points, as, e.g., transitions, the pulse has a bandwidth of ca. 60 Hz (20th harmonics). The amplifier bandwidth should be about 500 Hz if we want the signal to follow the temperature trend faithfully. On the other hand, if we want linear amplification of very small photocurrents, we need an FET amplifier. The AD645, with its gain bandwidth of 2 MHz, seems to be a good solution. To filter noise, we have placed capacitors of 10 pF across the feedback resistors. Since the biggest of them is 40 M Ω , the maximum time constant is 0.4 ms, which corresponds to a minimum bandwidth of 500 Hz, which is quite adequate.

Table I. Mid-Wavelength, Band, and Effective Wavelength of Each Channel of the Multiwavelength Pyrometer

| Channel No. | λ_m (nm) | $\Delta\lambda$ (nm) | λ_e (nm) |
|-------------|------------------|----------------------|------------------|
| 1 | 1025.0 | 49.8 | 1032.6 |
| 2 | 978.8 | 42.7 | 987.4 |
| 3 | 938.9 | 37.0 | 945.2 |
| 4 | 904.1 | 32.5 | 908.2 |
| 5 | 873.4 | 28.9 | 875.8 |
| 6 | 846.0 | 25.9 | 847.1 |
| 7 | 821.4 | 23.4 | 821.3 |
| 8 | 799.1 | 21.3 | 798.0 |
| 9 | 778.8 | 19.4 | 777.0 |
| 10 | 760.1 | 17.8 | 757.9 |
| 11 | 743.0 | 16.5 | 740.3 |
| 12 | 727.1 | 15.2 | 724.2 |
| 13 | 712.4 | 14.2 | 709.1 |
| 14 | 698.7 | 13.2 | 695.0 |
| 15 | 680.0 | 24.0 | 676.5 |
| 16 | 652.2 | 30.9 | 649.0 |
| 17 | 623.6 | 26.2 | 619.9 |
| 18 | 599.3 | 22.6 | 595.0 |
| 19 | 575.1 | 25.8 | 571.0 |
| 20 | 548.9 | 26.3 | 544.1 |

Although the channels are software selectable, a higher speed can be reached if unnecessary channels are suppressed in hardware. This can be achieved simply by inserting a card with the reduced number of channels. Another advantage of this architecture is the possibility of a quick change of the amplifier cards to meet special requirements of the experiment, e.g., higher speed with lower gain, achievable with the appropriate operational amplifiers.

No dedicated circuits for signal-to-temperature conversion are used, since all operations are performed in software on the basis of calibration data stored in a computer. Of course, in fast dynamic measurements, data are processed off-line.

3. EXPERIMENTAL SYSTEM

Modern techniques carry out experiments in physical systems (EXP in Fig. 3), in which sensors S_1, S_2, S_3, \dots are inserted measuring the physical quantities involved in the process. Signals properly conditioned are fed to

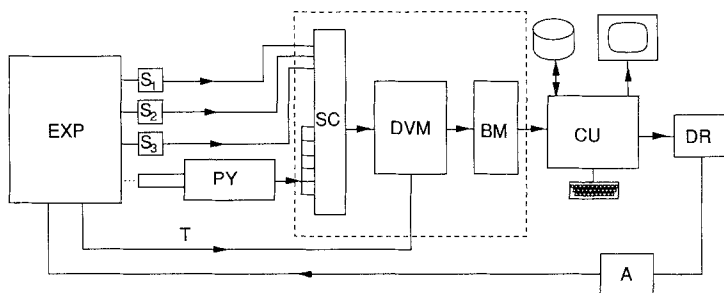


Fig. 3. Functional diagram of the experimental system.

an automatic data acquisition and control system (ADACS) which includes a processor (central unit CU) with its peripherals. Our pyrometer PY is one of the sensors, which presents up to 20 outputs to be connected to the ADACS.

The ADACS mounted in our laboratory is provided with all pieces of equipment required by the needs of our present research program. They are the following.

- (1) Two scanners, SC
 - (a) A high-precision, low-speed scanner, HP-S, made with low-thermal mercury wetted reed relays, with stray e.m.f. less than $1 \mu\text{V}$ and scanning speed reaching, with some voltmeters, 25 ms per operation
 - (b) A high-speed scanner, HS-S, with MOSFET switches allowing 100,000 operations/s.
- (2) Three digital voltmeters, DVM
 - (a) A high-precision digital voltmeter, HP-DVM, with 7.5 digits and accuracy 7×10^{-5} (this instrument, necessarily slow, with a speed of a few readings per second, is used mainly for calibrations, in connection with the local resistance and voltage standards)
 - (b) A medium-precision, medium-speed digital voltmeter, MP-DVM, with max. 6.5 digits, accuracy of 1×10^{-4} , 25 repetitions/s
 - (c) A high-speed, moderate-precision digital voltmeter, HS-DVM, with max. speed 100,000 readings/s, 10^{-3} accuracy, and 14-bit resolution.
- (3) A buffer memory, BM, with 64k data capacity.
- (4) Computer CU with the usual peripherals.

4. CALIBRATION

4.1. Pyrometer Wavelength Function (PWF)

The PWF is an instrument function, namely, the product of the spectral transmittance of the instrument and the spectral responsivity of the detector:

$$\Phi(\lambda) = \tau(\lambda) \sigma(\lambda) \quad (1)$$

Determination of this function, for all 20 channels, is performed automatically [3].

The pyrometer is aimed at the exit slit of a grating monochromator, while wavelengths are scanned from 500 to 1050 nm at narrow steps (ca. 1 nm) by driving the grating gear with a stepping motor controlled by the computer. All 20 channels are connected to the input terminals of the scanner HP-S and the outputs are measured by the precision voltmeter HP-DVM. Compensation for source power distribution and monochromator transmittance is performed by dividing each pyrometer reading by the value, at the same wavelength of the product of those quantities. A function proportional to this product is automatically determined by the same method, the only difference being the use of a thermal detector and wider monochromator slit. This function is given by cubic b-splines.

The PWF of each channel is stored in a file in numerical form as a table. The PWFs of channels 4 and 16 are represented in Fig. 4.

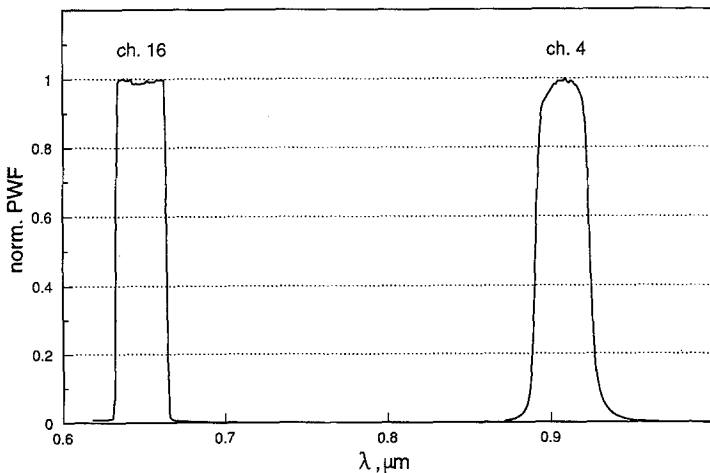


Fig. 4. Normalized pyrometer wavelength function (PWF) of channels 4 and 16.

The described procedure for determining the PWF requires not more than 45 min, with modest expenditure, and yields the same accuracy as in primary pyrometry.

4.2. Reference Temperature Signal

The signal at reference temperature is measured by scanning the pyrometer channels while it is focused on a blackbody cavity at one of the freezing points prescribed by the ITS-90. As fixed points are not now available in our laboratory, we temporarily circumvented this lack, by using a variable-temperature heat pipe blackbody cavity, whose temperature was measured by a Pt-PtRh 10% thermocouple calibrated by the IMGC, corrected to fit the ITS-90, and the high-precision DVM.

Pyrometer readings were taken from 1000 to 1300 K at 50 K intervals and they were fitted by the equation:

$$\ln S_i = a_{0,i} + a_{1,i}/T_i + a_{2,i}/T_i^2 \tag{2}$$

where $S = S/V$ is the dimensionless signal (voltage over volt), T is the Kelvin temperature, and subscript i refers to the channel number. Figure 5 shows how well data fit by this equation for channels 4 and 16.

Putting $T = 1337.33$ K into Eq. (2), we obtain the signals at the gold point, with an estimated temperature inaccuracy of 0.5 K. This is sufficient to test the present dynamic capabilities of our instrument.

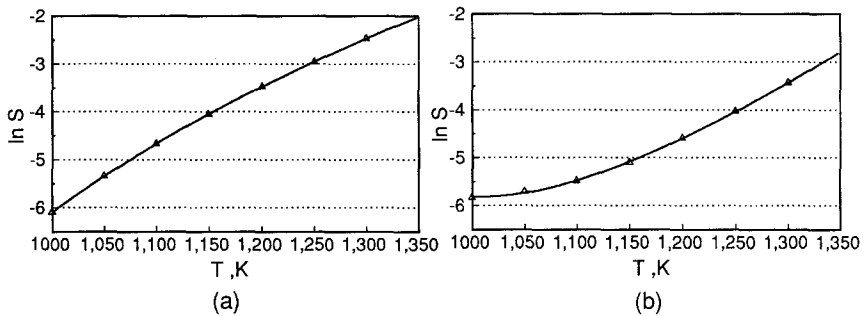


Fig. 5. The quantity $\ln S$ is a function of temperature for channels 4 (a) and 16 (b). The curves represent the fit according to Eq. (2).

4.3. Pyrometer Equation

The radiance temperature T_r can be calculated from the ratio Q between the signals at temperature T_r of the target and T_{Au} of the black-body at the gold point, according to the equation

$$Q = \int_{\Delta\lambda} \frac{\Phi(\lambda)}{\lambda^5 [\exp(C_2/\lambda T_r) - 1]} d\lambda \left\{ \int_{\Delta\lambda} \frac{\Phi(\lambda)}{\lambda^5 [\exp(C_2/\lambda T_{Au}) - 1]} d\lambda \right\}^{-1} \quad (3)$$

$\Phi(\lambda)$ and λ of each channel, previously stored in files, can be used to solve Eq. (3) numerically by iterations. But if we consider that one experiment may take up to 60,000 points, the calculations seem to be lengthy even for off-line processing. It is possible to speed up the treatment by applying to each channel a program developed for monochromatic pyrometers [4].

The signal ratio Q is calculated at fixed temperature steps, within a certain range, from Eq. (3). By fitting data of $\ln Q$ and $1/T_r$ by a second-degree polynomial, we obtain the following equation:

$$\ln Q = a_0 + a_1/T_r + a_2/T_r^2 \quad (4)$$

which, with proper range and bandwidth, yields T_r with a deviation not exceeding 0.01 K.

5. DYNAMIC TESTS

A pyrometric strip lamp was chosen to investigate the transient response of the multiwavelength pyrometer. The lamp was fed by a square current pulse. Instead of presetting the pulse time width, which could easily lead to the lamp destruction, we set the maximum current and limited the maximum lamp temperature, by presetting the maximum signal of one of the pyrometer channels (No. 4, which corresponds to the central wavelength of 900 nm).

The current pulse, generated by a power supply, preset at the desired current level, is triggered by a flip-flop and cut down by a voltage comparator and the same flip-flop. The same circuit provides a trigger to start the acquisition by the fast scanner and voltmeter. All data are stored in the buffer memory. This procedure allows the exploitation of the intrinsic speed of the system. When the process is over, the program continues by sending data to a file in the computer memory. Then row data can be processed and plotted as usual.

For each channel, 3000 temperature data points were taken, and at the end of each temperature scan, another channel read the instantaneous value of the lamp current. Thus 63,000 data were stored in the buffer memory at

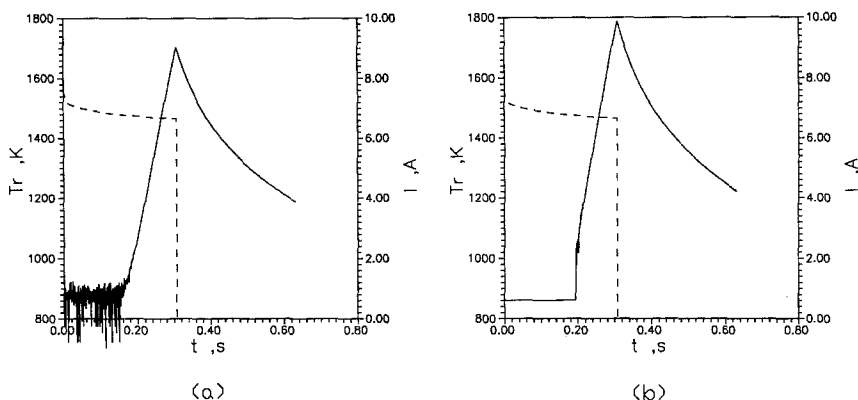


Fig. 6. Radiance temperature pulse of channels 4 (a) and 16 (b), superimposed on the current pulse.

a rate of 100 kHz. This frequency was checked with a calibrated signal generator. Radiance temperatures at two wavelengths are represented in Fig. 6. The noise of the diode array is such that only measurements above 900 K provide a meaningful signal-to-noise ratio.

6. CONCLUSION

A multiwavelength pyrometer has been successfully applied to transient temperature measurement with 200- μ s resolution when operated at 20 wavelengths. By reducing their number, the resolution may be improved in inverse proportion. Its particular technique of selecting the bandwidths makes them intrinsically stable. Our instrument allows an easy choice of the operating wavelength and presents some advantages over previously designed instruments of this kind.

ACKNOWLEDGMENT

The authors wish to acknowledge the help of Mr. L. Cascioli in designing part of the electronic circuit.

REFERENCES

1. G. Ruffino, *Int. J. Thermophys.* **13**:165 (1992).
2. G. Ruffino, Chu Zaixiang, Kang Songgao, and Dai Jingmin, in *Temperature Its Measurement and Control in Science and Industry, Vol. 6*, J. F. Schooley, ed. (American Institute of Physics, New York, 1992), p. 807.
3. P. Coppa, G. Ruffino, and A. Spena, *High Temp. High Press.* **20**:479 (1988).
4. G. Ruffino, *High Temp. High Press.* **14**:393 (1984).

NOTE ADDED BY THE EDITOR

Professor Giuseppe Ruffino died shortly after submitting the final version of this paper. It is unfortunate that he could not see the publication of his paper, which constitutes a valuable addition to his impressive list of publications on pyrometry.